

Microwave-enhanced cracking over ZSM-5 (20) catalysts: Taguchi optimization for improved conversion and energy savings

Muataz M. Sulaiman^{1*}, Hasan F. Makki²

^{1,2}Department of Chemical Engineering, University of Baghdad; muataz.sulaiman1507d@coeng.uobaghdad.edu.iq (M.M.S.)
drhasanf.m@coeng.uobaghdad.edu.iq (H.F.M.).

Abstract: For heavy naphtha cracking, the combination of microwave irradiation and ZSM-5 (20) catalyst increases conversion and saves energy. The QVF tube reactor is 240 mm long, 12.7 mm inner diameter with an 80 mm effective zone. The feed goes into the reactor after it has been heated, and the reaction takes place in the catalytic zone, where ceramic particles loaded in the bottom and upper regions of the tube help the feed components and products spread out more evenly. All products were condensed and analysed using gas chromatography. The cracking was done under the following conditions: microwave irradiation (750–1250 W), preheating temperatures (150–250 °C), and space velocities (2 and 6 l/hr). The microwave radiation generates hot spots in the catalyst structure, which enhance cracking. The best conversion is (66.77%) at a microwave power of 1250 W, a flow rate of 2 l/hr, and a preheating temperature of 200 °C. The nitrogen injection increased conversion in all conditions. Conventional techniques are incapable of cracking heavy naphtha within the temperature range of 150–250 °C. Generally, an increase in microwave power and preheating temperature leads to an increase in conversion, while a decrease in flow rate, both with and without nitrogen injection, negatively impacts conversion. This study examined the impact of microwave radiation with a catalyst on residence duration, energy efficiency, and conversion at lowered temperatures.

Keywords: Catalytic cracking, Cracking reactor, Heavy naphtha, Microwaves and heterogeneous catalysis, Microwaves.

1. Introduction

Naphtha consists of several hydrocarbon compounds ranging from C₄ to C₁₂, mostly including n-paraffins, isoparaffins, and naphthenics (1). The concentration of the primary components exhibits significant variation, contingent upon the source of petroleum and the operational parameters of the refinery (2)(3).

The catalytic cracking of naphtha, which consists of n-alkanes with carbon chain lengths ranging from C₄ to C₁₂, takes place under conditions of high operational temperature (4). The process involves high reaction temperatures and significant steam quantities in the feed to enhance the yield of ethene and propene (5). ZSM-5 zeolites can be used with various chemical compositions (6). The technique allows us to examine the impact of catalyst activity, as well as its progression over time. This also provides information on the possible reversible and irreversible deactivation of the catalyst (7).

Naphtha catalytic cracking is a promising alternative to thermal cracking. In contrast to the thermal process, catalytic cracking consumes less energy and generates greater propylene and ethylene yields at lower temperatures (8). In catalytic cracking, various catalysts in the form of solid particulates such as zeolite, aluminum hydrosilicate, bauxite, silica-alumina, and metals are introduced (9).

Zeolites, specifically ZSM-5, have high catalytic activity and act as effective catalysts and supports for many processes, including cracking, alkylation, aromatisation, and isomerisation of hydrocarbons (10). This is primarily due to their activity and ability to select and shape the molecules involved (11). The fundamental interactions between microwaves and catalysts in naphtha cracking have been investigated. When compared with conventional heat sources, microwave energy has a significant

impact on many chemical reactions (12). Microwave irradiation has numerous advantages, including a short reaction time, a low reaction temperature, a short start-up time, low cost, accurate process control, and high energy efficiency (13). There are two distinct components to the microwave heating technique: electrical energy, which is transformed into microwave energy, and microwave energy, which is converted into effective heat (14).

Some researchers compared the amount of energy required for chemical reactions when using microwaves versus conventional methods and found that microwaves' chemical activity is energy (10–1000) times faster than conventional heating (15). Microwave technology has gained popularity and is generally regarded as a technological advancement in this field because it can increase the rate of many chemical reactions (16). Some research suggests that the microwave's effectiveness may be related to the electromagnetic effect, which has been associated with the selective absorption of energy by polar molecules (17).

Moreover, microwave-assisted reactions are generally more rapid and produce superior results relative to conventional methods. The illustrated microwave enhanced yields of the desired aromatic product and reduced the presence of environmentally harmful compounds (12). Due to substantial energy consumption, the hydrocarbon processing sector of the chemical industry consistently attempts to improve the efficiency of its processing methods (18). Because of its efficient energy transfer mechanisms, microwave power for direct material heating is rapidly emerging as a vital resource for many industrial processes (19). The primary goal is to determine the optimal conditions for the efficient and successful application of microwave technology in heavy naphtha cracking.

The application of microwave power is preferred for naphtha cracking due to its capability to operate at lowered temperatures, produce greater conversion rates, and consume less energy; this is one of our conclusions on microwave-assisted cracking. The study discusses the correlation between microwave power, flow rate, and preheating temperature. All previous studies have not enhanced the results by changing the previously mentioned parameters within the specified limits.

2. Materials

2.1. Feedstock

The heavy naphtha was used as a raw material for the catalyst cracking process with an initial and final boiling point of 80°C to 185°C. The naphtha is produced in the Al-Najaf refinery, which applies the atmospheric fractional distillation. Table 1 shows the heavy naphtha analysis performed by Basra Oil Company.

Table 1.
PONA analysis of heavy naphtha.

Composition	Wt. %
n-Paraffin	31.026
i-Paraffin	33.258
Naphthene	10.003
Aromatic	18.938
Olefine	1.169
Undefined	5.606

2.2. ZSM-5 Catalyst

The catalyst type ZSM-5(20) exhibits a spherical shape, with particles ranging in size from 2 to 3 mm, and a silicon-to-aluminum ratio of 20:1 mol. (Congyi City Meiqi Industry and Trade Co., China)

2.3. Nitrogen Gas

The flow of nitrogen (30 cm³/min) started 15 min before the beginning of the experiment. The nitrogen reactivates the catalyst.

3. Experimental Method

3.1. The Catalytic Cracking Unit

The system was established as a continuous flow with a heavy naphtha catalytic reactor. The process equipment includes a feedstock drum, feed pump, electrical preheater, microwave oven, QVF tubular reactor, cooling and condensation system, separator, gas flow meter, one-way valve, and electrical power cabinet, as illustrated in Figure 1.

The feedstock is stored in the feed tank and then pushed through the heating element to the reactor, which is located in the microwave oven's core. The effluent from the reactor enters the condenser, where some substances are condensed while others are released into the atmosphere. The condensate product was collected and subsequently analysed using gas chromatography.

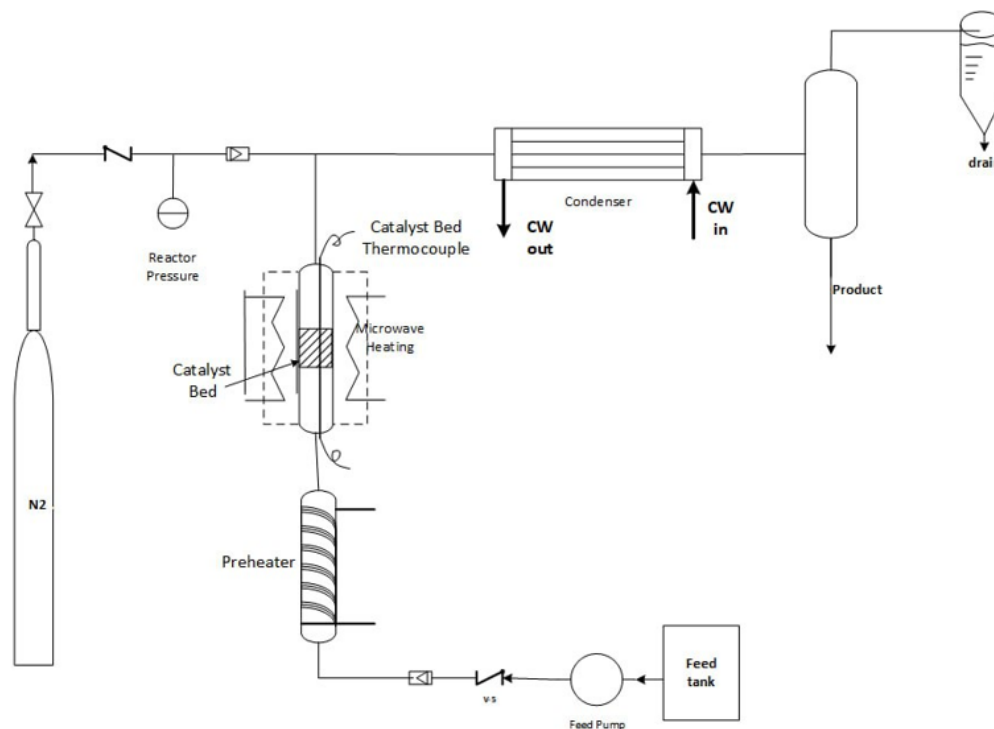


Figure 1.
The catalytic cracking unit process flow diagram.

3.2. Reactor

A QVF tube with 12.7 mm inner diameter and 240 mm reactor length within the microwave effective zone was used as a reactor. Inside the microwave oven, the reactor has three packing zones with a height of 80 mm. The catalyst was packed in the middle zone, while the other zones were filled by inert ceramic particles with an average diameter of 5 mm to prevent channelling and improve distribution, as illustrated in Figure 2.



Figure 2.
The reactor's three equal packing zones.

4. Characterization of the ZSM-5 Catalysts

The catalyst evaluation required various chemical, physical, and microstructural characteristics.

4.1. XRD

Figure 3 shows the XRD patterns of the zeolite ZSM-5 (20). The narrow, high-intensity peaks in the zeolite samples suggest that the zeolite ZSM-5 (20) samples exhibit high crystallinity. XRD analysis of zeolite demonstrates that there is a sharp peak that refers to quartz and also refers to free quartz in the zeolite powder. The corresponding values reported for ZSM-5 (20) (Sodium Aluminium Silicate) match the chemical formula ($\text{Na}_2 \text{Al}_{1.9} \text{Si}_{94.1} \text{O}_{192}$) found in JCPDS, Card No. 00-048-0136, as illustrated in Figure 3.

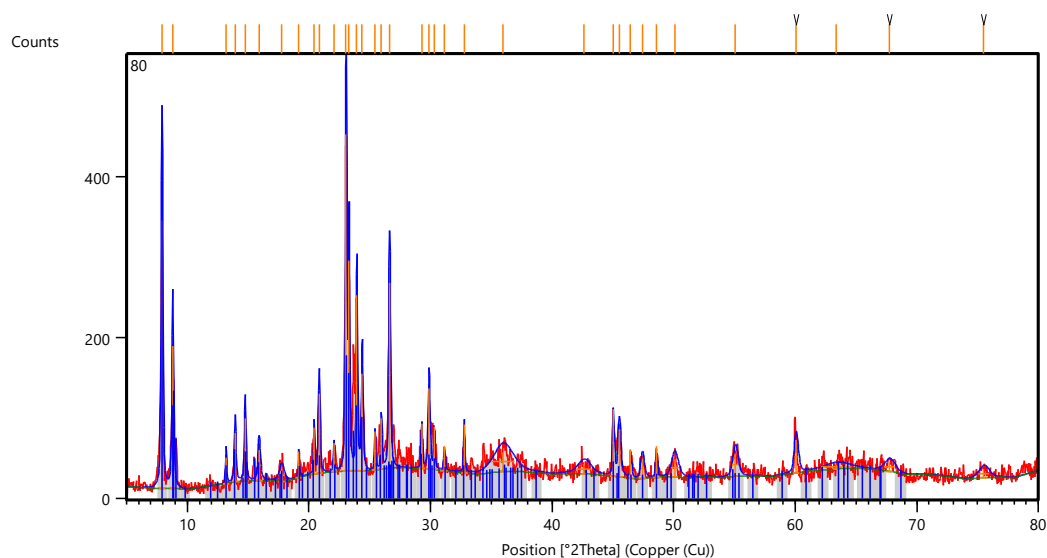


Figure 3.
The XRD patterns of the Zeolite ZSM-5 (20) powders.

4.2. SEM

Crystal forms, external surfaces, and purity of the phases are shown in SEM micrographs with magnification (10, 25, 50, and 200 kx), Figure 4. The hexagonal crystal shape has dimensions (25.57 nm) that control the crystal's growth. Additionally, crystal size distribution phenomena are attributed to aggregation, twinning, and sometimes intergrowth. At a lower magnification value, we detected indications of single crystals.

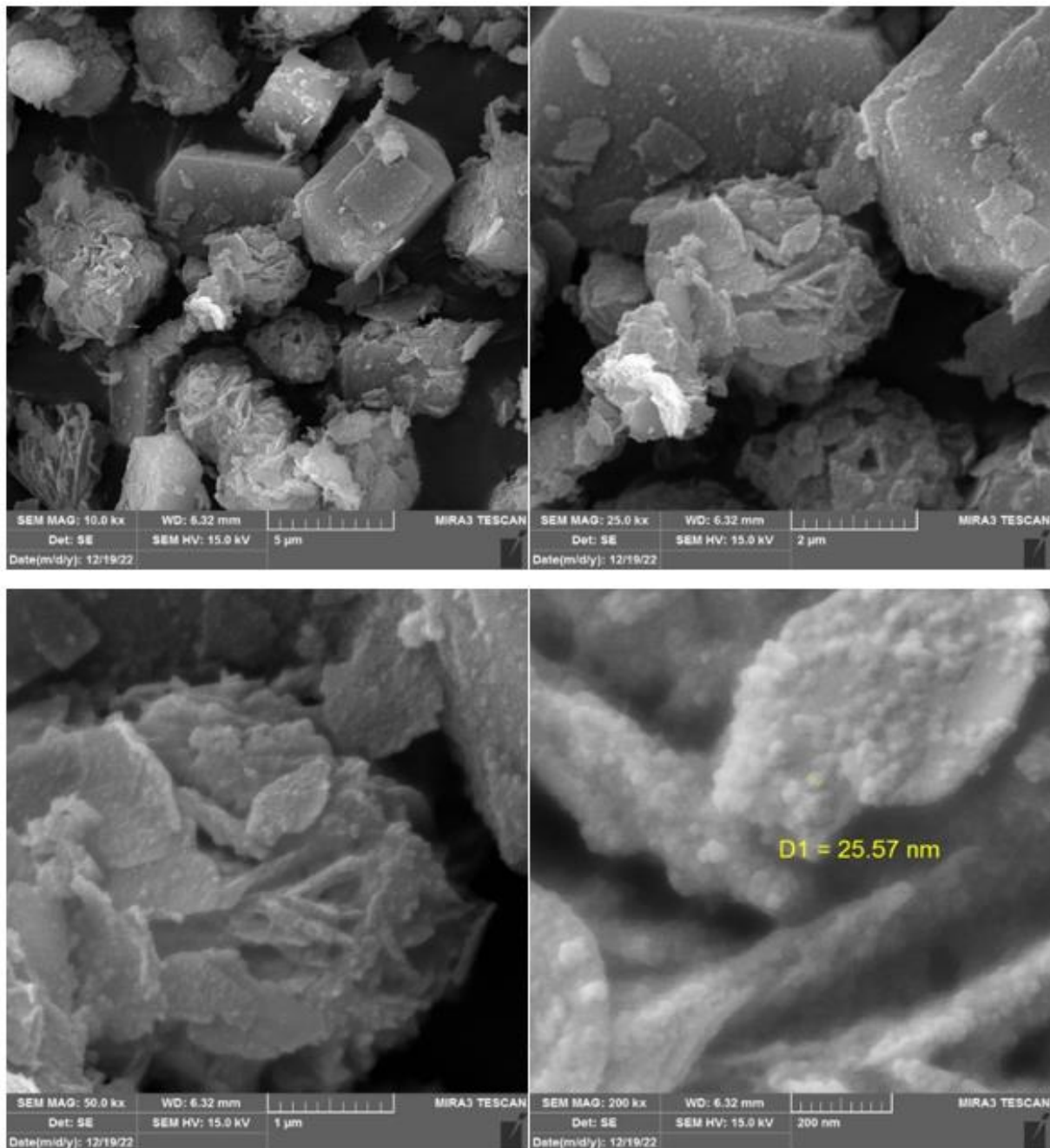


Figure 4.
The micrographs of ZSM-5 (20).

4.3. Surface Area and Pore Volume

Nitrogen physical adsorption using the BET method measures the specific surface area and total pore volume of ZSM-5(20). Increasing (SSA) of zeolite ZSM-5(20) caused by increasing the combined total pore volume which gives higher cracking rate. Moreover, the ZSM-5(20) show type IV isotherms with distinguishing hysteresis loops corresponding to mesoporous materials according to (IUPAC) classification of adsorption isotherms that shown in Figures 5 and 6. Adsorbed volume increases at higher p/p_0 as well as a hysteresis loop. A non-distinct increase of adsorbate volume in the low p/p_0

region in type IV isotherms indicates the absence of the micropores. The increase in adsorbed volume at higher p/p_0 in type IV isotherms is caused by capillary condensation below the expected condensation pressure of the adsorbate. Capillary condensation is a secondary process that requires the preformation of an adsorbed layer on the pore walls which formed by multilayer adsorption. Both processes generally occur simultaneously in range of 0.3-1 p/p_0 (Table 2).

Table 2.
The results of surface area test.

Sample code	SBET (m^2/g)	Pore volume (V_p) (cm^3/g)
20	245.11	0.2791

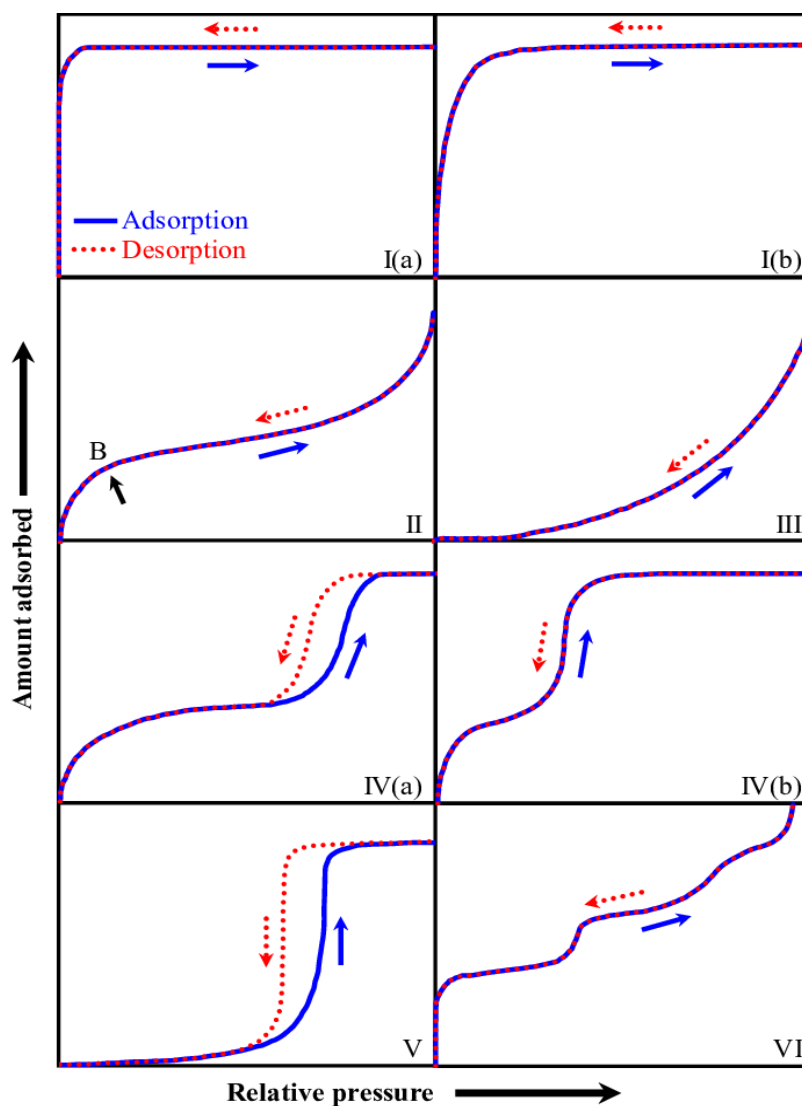


Figure 5.
IUPAC classification of Adsorption/desorption isotherms of N_2 at 77°K .

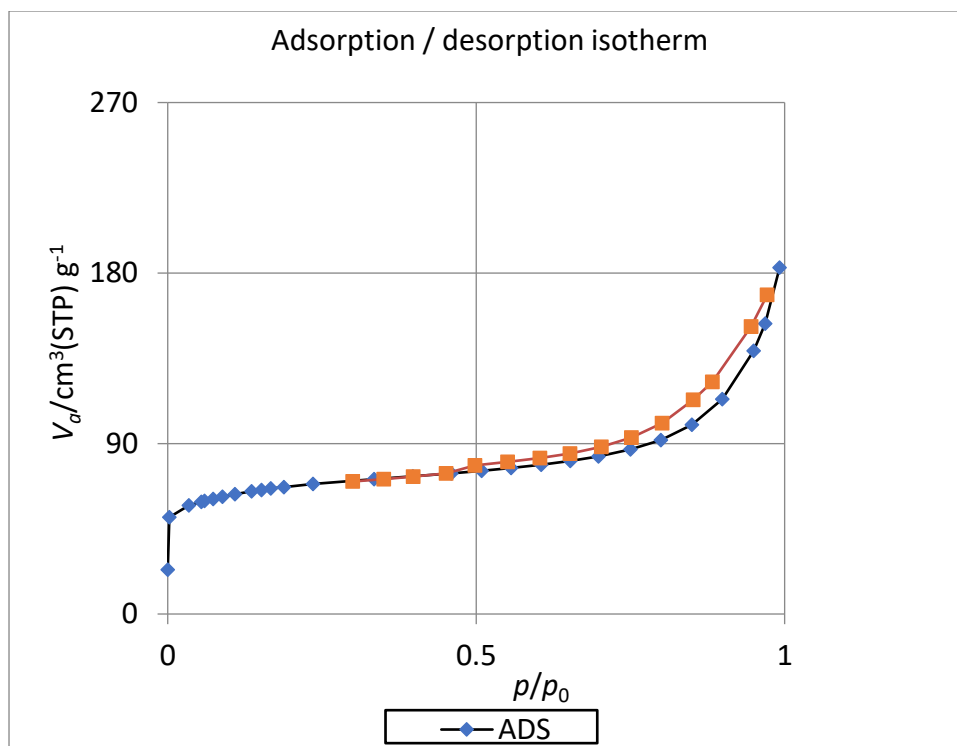


Figure 6.
Adsorption/desorption isotherms of N₂ at 77°K of ZSM-5 (20).

4.4. Fourier-Transform Infrared Spectroscopy (FTIR)

The organization of zeolite's structures is used to determine the different chemical groups present on the catalysis surface. Secondary building units (SBU) are formed from primary building units (PBU) of zeolites, which are tetrahedra linked by oxygen bridges. This study looked at the infrared (FTIR) spectrum of zeolites that belonged to these structural groups. It was called the relationship between SBU type and vibrational spectrum. We observed a spectrum range between 400 and 4000 cm⁻¹. It is a technique that primarily investigates the catalyst at the molecular level.

The bands that appear in the region between 3214 and 3845 cm⁻¹ reveal the OH stretching band, also known as the low frequency band, SiO₄ molecules, and Al-OH recognizing the ZSM-5 structure. The bands in the range of 1010–1019 cm⁻¹ denote Si-O. The absorption peak in the range 412–448 cm⁻¹ was assigned to Si-O-Al stretching, where Al is in octahedral coordination. The vibration of Si-Al groups represents external asymmetrical stretching, while the band at range 613–625 cm⁻¹ leads to internal tetrahedral symmetrical stretching, as shown in figure 7. Therefore, we found that the FTIR of the ZSM-5 (20) conforms to the typical absorption peaks of synthesis, as previously mentioned (20).

The FTIR spectra of ZSM-5 (20) showed a sharp and high intensity of the hydroxyl (OH) band zeolite in the region (411–1081) cm⁻¹, as depicted in Figure 7. The OH groups, bridging Si and Al atoms, displayed strong Bronsted acid properties in the region between 3560 and 3630 cm⁻¹, as shown in Figure 7. The interaction between Bronsted acid sites and widely spread Lewis sites (aluminium species) made the proton acidity higher (21).

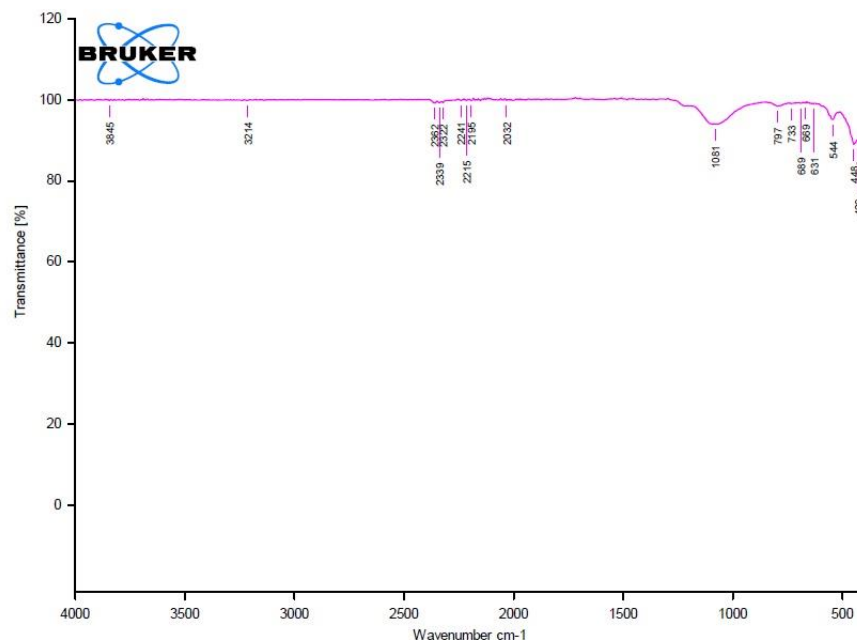


Figure 7.
IR spectra of ZSM-5 (20).

4.5. X-Ray Fluorescence (XRF) Analysis

The XRF technique analyzed the quantitative chemical compositions of the zeolite ZSM-5(20), which facilitates chemical phase identification and chemical structure evaluation by FTIR. Table 3 lists the chemical composition as a percentage of weight.

Table 3.

The zeolite [ZSM-5(20) XRF analysis results].

SiO ₂ %	Al ₂ O ₃ %	Na ₂ O %	K ₂ O %	CaO %	MgO %	Fe ₂ O ₃ %	TiO ₂ %	SO ₃ %	MnO %	P ₂ O ₅ %	Cl %	LOI %
84.432	4.389	0.652	0.567	1.079	2.88	1.804	0.352	0.029	0.045	0.078	0.282	3.36

It was observed that the percent of SiO₂ (84.432%) is dominant in zeolites ZSM-5 (20), while the second highest percentage is Al₂O₃ (4.389%). The different compositions are due to industrial and production variables. Si/Al influences the morphology and characteristics of zeolites.

5. Cracking of Heavy Naphtha

The heavy naphtha was analyzed by PIONA (paraffin, i-paraffin, olefin, naphthene, aromatic) according to ASTM D5134 standard. A gas chromatograph (MS-GC manufactured by Agilent) was employed to evaluate the reaction conversion. When different microwave power, preheating temperature, flow rate, and SiO₂/Al₂O₃ ratios were used in ZSM-5 catalysts (20), heavy naphtha was cracked by them. The cracking of heavy naphtha compounds is mostly represented by the conversion of paraffins to aromatics and olefins. The catalytic cracking reactions were performed with and without N₂ injection.

5.1. ZSM-5 (20) Catalysts

Two sets of experiments were used to look into the reaction conversion of heavy naphtha, one with nitrogen injection and one without. The response for the Taguchi method of reaction conversion was measured after a 12-minute period for each set of control variables as shown in Table 4.

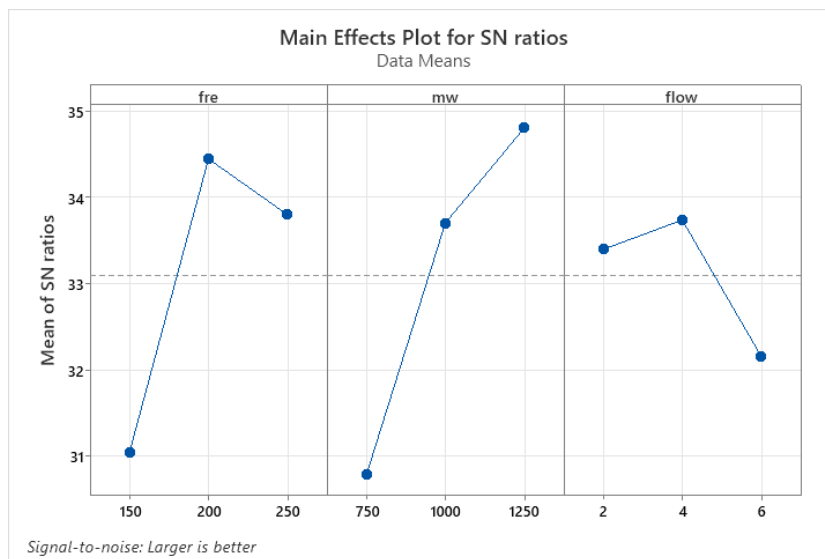
Table 4.
Conversion of paraffin of Taguchi's OA for zeolite ZSM-5 (20).

Preheating (°C)	Microwave (W)	Flowrate (l/hr)	Conversion without N ₂ injection	Conversion with N ₂ injection
150	750	2	21.737	28.321
150	1000	4	33.043	41.378
150	1250	6	32.363	38.809
200	750	4	33.169	43.328
200	1000	6	42.477	50.790
200	1250	2	59.540	66.767
250	750	6	24.599	33.846
250	1000	2	47.940	54.122
250	1250	4	56.301	64.182

Figure 8 explains the interaction effect of the variables (with and without nitrogen injection) on the conversion of paraffin into signal-to-noise ratios. Figure 8, The preheating temperature maximises the (S/N) ratio up to 200 C° and decreases in the interval between A2 and A3, where the (S/N) values are 34.45 to 33.8 with nitrogen injection and 32.82 to 32.15 without nitrogen injection. As microwave power increased, paraffin conversion increased from 28.33 at B1 to 33.57 at B3 (without nitrogen injection) and 30.79 at B1 to 34.81 at B3 (with nitrogen injection). The (S/N) ratio decreased as the flowrate increased for experiments without nitrogen injection; the (S/N) value decreased from 31.95 at C1 to 30.19 at C3, while it increased up to C2, then decreased from 33.74 at C2 to 32.16 at C3 for experiments with nitrogen injection. It was discovered that the reaction conversion has the same trend for experiments with and without nitrogen injection for preheating temperature and microwave power, while the flowrate has a different behaviour.



A: Without nitrogen injection



B: With nitrogen injection.

Figure 8.

The signal to noise ratio for preheating, microwave power, and flow rate at zeolite ZSM-5 (20) A: without nitrogen injection, B: with nitrogen injection.

The maximum *p* value obtained is less than 0.05, so it is significant for microwave power, preheating temperature, and flowrate (without nitrogen injection) with *p* values (0.002, 0.003, and 0.012, respectively) according to table 5. The *p* value (with nitrogen injection) has better compatibility and control variable rank according to Table 6 as follows (preheating temperature, microwave power, and flowrate with *p* values of 0.000, 0.000, and 0.002, respectively).

Table 5.
Analysis of variance for SN ratios at zeolite ZSM-5 (20).

Source	Without nitrogen injection						Without nitrogen injection				
	DF	Seq SS	Adj SS	Adj MS	F	P	Seq SS	Adj SS	Adj MS	F	P
Preheating	2	23.4996	23.4996	11.7498	311.84	0.003	19.5054	19.5054	9.7527	2116.17	0.000
mw	2	44.3131	44.3131	22.1566	588.04	0.002	25.8525	25.8525	12.9263	2804.77	0.000
Flow	2	6.1206	6.1206	3.0603	81.22	0.012	4.1408	4.1408	2.0704	449.25	0.002
Residual error	2	0.0754	0.0754	0.0377			0.0092	0.0092	0.0046		
Total	8	74.0087					49.5080				

Table 6.
Response table for signal to noise ratios at zeolite ZSM-5 (20).

Level	Without nitrogen injection			Without nitrogen injection		
	Preheating	mw	Flow	Preheating	mw	Flow
1	29.11	28.33	31.95	31.05	30.79	33.40
2	32.82	32.19	31.94	34.45	33.71	33.74
3	32.15	33.57	30.19	33.80	34.81	32.16
Delta	3.72	5.24	1.76	3.40	4.02	1.58
Rank	2	1	3	2	1	3

The correlation equation of reaction conversion, when combined with control variables, exhibits a greater influence from interaction variables than from individual variables. Fitting the experimental conversion data has an R^2 value of 99.59% (without nitrogen injection). The Taguchi method proposes

regression correlation analyses of OA, which represent the control variables versus the reaction conversion (Equation 1).

$$\text{Conv. \%} = 12.467 - 0.46B - 4.7e^{-2}A + 39.4C + 8.27e^{-4}AB - 0.085BC - 0.022AC \quad 1$$

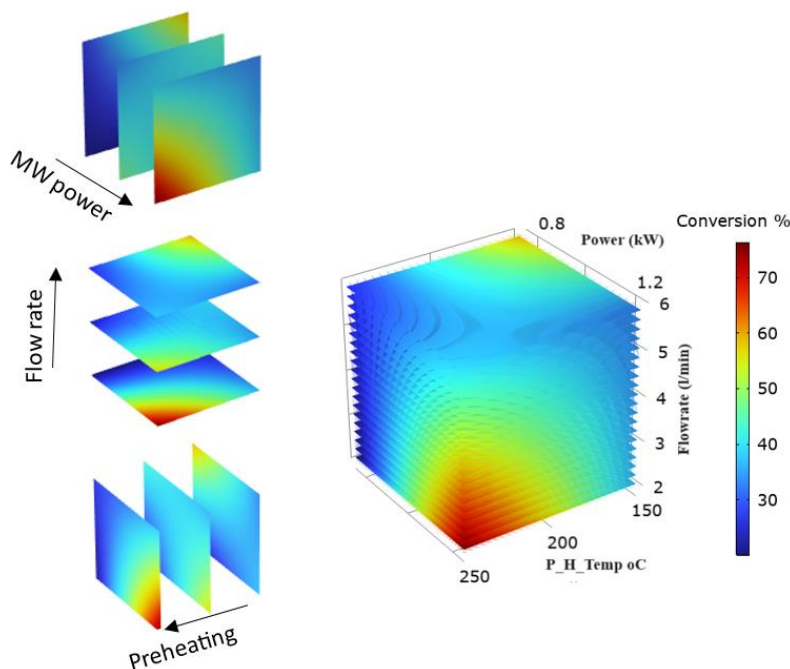
The Taguchi method's polynomial equation (Equation 2) represents the controlled variables (with nitrogen injection). The formulated equation has an R^2 value equal to 98.93%, which indicates a good fit.

$$\text{Conv. \%} = 25.28 - 0.556B - 0.0602A + 46.146C + 9.5e^{-4}AB - 0.095BC - 0.0264AC \quad 2$$

Figure 9 illustrates the reaction conversion increased with increasing preheating temperature and microwave power at constant flowrate. The reaction conversion decreased with increasing flowrate using the ZSM-5 (20) catalyst, both with and without nitrogen injection.

The preheating temperature effect on the reaction conversion within the range 150–200 °C (increased the conversion). The conversion decreased above 200 °C due to catalyst poisoning. The experiment with nitrogen injection resulted in a higher reaction conversion compared to the experiment without nitrogen injection, primarily due to a decrease in poisoning and an increase in velocity (mobility of molecules). The flowrate consistently decreases with residence time, resulting in a decrease in the reaction conversion when nitrogen injection is not used. The reaction conversion at the range 150–200 °C almost has the same value because of the interaction effect between the flowrate, preheating, and nitrogen injection, which reactivate the catalyst.

The microwave power has a great effect on conversion, and it is increasing in the range 750–1250 W. The microwave power creates a hot spot, increasing the catalyst's activity and the reaction's activation energy. When 1250 W of microwave power, 2 l/hr of flowrate, and 200 °C of preheating temperature are combined, they give the best conversion (59.54%) without nitrogen injection and 66.77 % with nitrogen injection. It could be concluded that the reaction conversion is higher with nitrogen injection than without nitrogen injection.



A

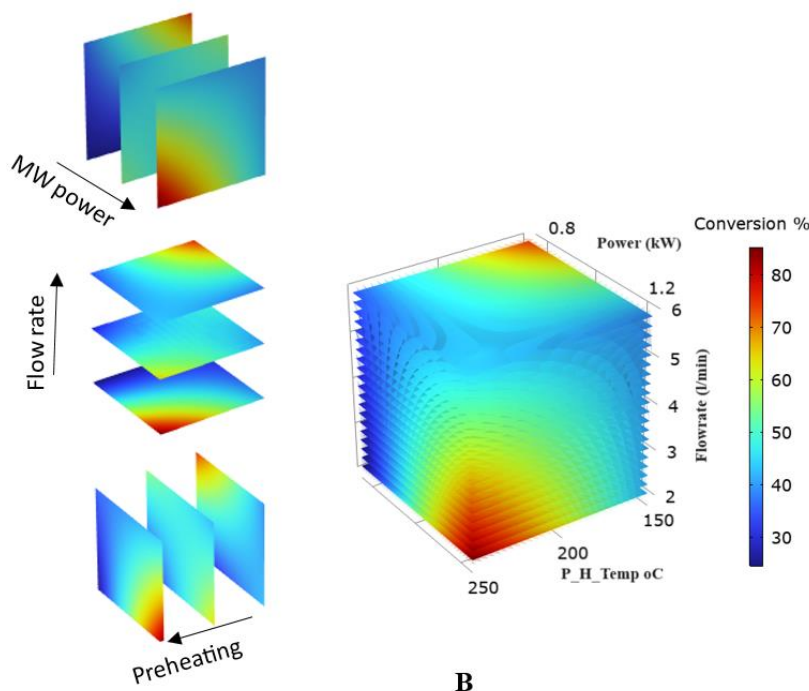


Figure 9.
3D representation and the projections of a regression equation, A: (1), B: (2).

6. Conclusion

The cracking process needs energy and excellent selectivity. It could be achieved with catalysis and microwave power. The effect of microwave power, which generates hot spots, increases the conversion, reaction rate, and energy savings. The addition of nitrogen injection gives better products and a higher reaction rate. The optimal conversion rate of the cracking process is 66.77% at a microwave power of 1250 W, a flow rate of 2 l/hr, and a preheating temperature of 200 °C. The flow rate negatively affects the range of 4 to 6 l/h, while it has no effect within the range of 2 to 4 l/h. Conventional techniques are incapable of cracking heavy naphtha within the temperature range of 150–250 °C.

Copyright:

© 2024 by the authors. This article is an open access article distributed under the terms and conditions of the Creative Commons Attribution (CC BY) license (<https://creativecommons.org/licenses/by/4.0/>).

References

- [1] Abdullah NM, Hussien HQ, Jalil RR. Heavy Naphtha Desulfurization by Ozone Generated via the DBD Plasma Reactor. *Iraqi J Chem Pet Eng.* 2024;25(2):131–7.
- [2] Hammadi AN, Shakir IK. Enhancement the octane number of light naphtha by adsorption process. *AIP Conf Proc.* 2020;2213(March).
- [3] Da Silva VH, Reboucas M V., Salles AR, Pimentel MF, Pontes MJC, Pasquini C. Determination of naphtha composition by near infrared spectroscopy and multivariate regression to control steam cracker processes. *Fuel Process Technol* [Internet]. 2015;131:230–7. Available from: <http://dx.doi.org/10.1016/j.fuproc.2014.10.035>
- [4] A.K. Mohammed AH, Karim S, M. Rahman A. Characterization and Cracking Activity of Zeolite Prepared from Local Kaolin. *Iraqi J Chem Pet Eng.* 2010;11(2):35–42.
- [5] Abd MF, Al-yaqoobi AM, Abdul-Majeed WS. Catalytic Microwave Pyrolysis of Albizia Branches Using Iraqi Bentonite Clays. *Iraqi J Chem Pet Eng.* 2024;25(2):175–86.
- [6] Al-Jubouri SM, Al-Jendeel HA, Rashid SA, Al-Batty S. Green synthesis of porous carbon cross-linked Y zeolite nanocrystals material and its performance for adsorptive removal of a methyl violet dye from water. *Microporous Mesoporous Mater* [Internet]. 2023;356:112587. Available from: <https://www.sciencedirect.com/science/article/pii/S1387181123001580>
- [7] Corma A, Mengual J, Miguel PJ. Steam catalytic cracking of naphtha over ZSM-5 zeolite for production of propene

- and ethene: Micro and macroscopic implications of the presence of steam. *Appl Catal A Gen* [Internet]. 2012;417–418:220–35. Available from: <http://dx.doi.org/10.1016/j.apcata.2011.12.044>
- [8] Katada N, Kageyama Y, Takahara K, Kanai T, Ara Begum H, Niwa M. Acidic property of modified ultra stable Y zeolite: increase in catalytic activity for alkane cracking by treatment with ethylenediaminetetraacetic acid salt. *J Mol Catal A Chem* [Internet]. 2004;211(1):119–30. Available from: <https://www.sciencedirect.com/science/article/pii/S1381116903006915>
- [9] Falcone G, Hewitt G, Alimonti C. *Multiphase Flow Metering: Principles and Applications*. 2009.
- [10] Ahmedzeki NS, Alhassani MH, Al-Mayah AMR, Rashid HA. The use of locally prepared Zeolite (Y) for the removal of hydrogen sulfide from Iraqi natural gas. *Res J Pharm Biol Chem Sci*. 2016;7(6):1526–35.
- [11] Mohiuddin E, Mdleleni MM, Key D. Catalytic cracking of naphtha: The effect of Fe and Cr impregnated ZSM-5 on olefin selectivity. *Appl Petrochemical Res*. 2018;8(2):119–29.
- [12] Abd M, Al-yaqoobi A. The feasibility of utilizing microwave-assisted pyrolysis for Albizia branches biomass conversion into biofuel productions. *Int J Renew Energy Dev*. 2023 Oct 17;12.
- [13] A.M. Mohammed S, K. Salih W. Microwave Assisted Demulsification of Iraqi Crude Oil Emulsions Using Tri-octyl Methyl Ammonium Chloride (TOMAC) Ionic Liquid. *Iraqi J Chem Pet Eng*. 2014;15(3):27–35.
- [14] Wang W, Zhao C, Sun J, Wang X, Zhao X, Mao Y, et al. Quantitative measurement of energy utilization efficiency and study of influence factors in typical microwave heating process. *Energy* [Internet]. 2015;87:678–85. Available from: <https://www.sciencedirect.com/science/article/pii/S0360544215006179>
- [15] Mozafari M, Nasri Z. Operational conditions effects on Iranian heavy oil upgrading using microwave irradiation. *J Pet Sci Eng* [Internet]. 2017;151(December 2016):40–8. Available from: <http://dx.doi.org/10.1016/j.petrol.2017.01.028>
- [16] Gawande MB, Shelke SN, Zboril R, Varma RS. Microwave-Assisted Chemistry: Synthetic Applications for Rapid Assembly of Nanomaterials and Organics. *Acc Chem Res* [Internet]. 2014 Apr 15;47(4):1338–48. Available from: <https://doi.org/10.1021/ar400309b>
- [17] Hoz A, Díaz-Ortiz A, Moreno A. Microwaves in Organic Synthesis. Thermal and Non-Thermal Microwave Effects. *Chem Soc Rev*. 2005 Mar 1;34:164–78.
- [18] Mora M, del Carmen García M, Jiménez-Sanchidrián C, Romero-Salguero FJ. Transformation of light paraffins in a microwave-induced plasma-based reactor at reduced pressure. *Int J Hydrogen Energy*. 2010;35(9):4111–22.
- [19] Mohammed SAM, Mohammed MS. The Application of Microwave Technology in Demulsification of Water-in-Oil Emulsion for Missan Oil Fields. *Iraqi J Chem Pet Eng* [Internet]. 2013;14(2):21–7. Available from: www.iasj.net
- [20] Kordatos K, Gavela S, Ntziouni A, Pistiolas KN, Kyritsi A, Kasselouri-Rigopoulou V. Synthesis of highly siliceous ZSM-5 zeolite using silica from rice husk ash. *Microporous Mesoporous Mater*. 2008;115(1–2):189–96.
- [21] Hubbard PS and AT. No Title. In: *Encyclopedia of Surface and Colloid Science*. 2nd ed. Taylor & Francis, New York; London; 2006. p. 1148–50.